Maxwell Cattaneo double diffusive convection (DDC) in a viscoelastic fluid layer

Monal Bharty[1], Atul. K. Srivastava[2], Hrisikesh Mahato[3]
Department of Mathematics, School of Natural Sciences,
Central University of Jharkhand,
Ranchi−825305, India
Emails: priyabharty58@gmail.com[1], atulshaswat@gmail.com[2]
hrishikesh.mahato@cuj.ac.in[3]

December 28, 2022

Abstract

The onset of Maxwell-Cattaneo DDC in a viscoelastic fluid layer is studied using linear stability analysis with the help of normal mode technique. The parabolic advection diffusion equation, which presupposes classical fickian diffusion for both heat and salt, controls the evaluation of temperature and salinity. Analytically, the onset criteria for stationary and oscillatory convection is derived. Since the onset of stationary (steady case) convection is unaffected by Maxwell-Cattaneo effects as well as visco-elastic parameters, oscillatory convection rather than stationary convection is the key to visualize the effects of different parameters in this paper. Two different scenarios for oscillatory convection have been discussed (i) when Maxwell-Cattaneo coefficient for salinity $C_S = 0$ and (ii) when Maxwell-Cattaneo coefficient for temperature $C_T = 0$. Also a comparative study for these two cases i.e. $C_S = 0$ and $C_T = 0$ is performed for different controlling parameters like relaxation parameter (λ_1), retardation parameter (λ_2), diffusion ratio (τ), solutal Rayleigh number (Ra_S) and Prandtl number (Pr) with the help of graphs.

Keywords

DDC, Maxwell-Cattaneo Effect (M-C Effect), Viscoelastic binary fluid, Rayleigh number, Thermal Convection.

1 Introduction

The viscoelastic fluid flow is of significant importance in many fields of science, engineering, and technology, including geophysics, bioengineering, and the

processing of materials in the nuclear, chemical, and petroleum sectors [15][4]. Unique patterns of instabilities, such as overstability, which cannot be predicted or seen in Newtonian fluid, are present in viscoelastic fluids. For almost 40 years [5], the literature has explored the nature of convective motions in a thin horizontal layer of viscoelastic fluid heated from below in the context of the classical Rayleigh-Benard convection geometry. The key papers by Vest and Arpaci [5] provided the first thorough study of the linear stability of a layer of an upper-convected Maxwell fluid, in which stress exhibits an elastic response to strain typified by a single viscous relaxation period. Due to the high viscosity of the polymeric fluids, flow instability and turbulence are much less common than in Newtonian fluids. For a very long time, it has been widely accepted that in realistic experimental conditions, oscillatory convection cannot occur in viscoelastic fluids .However, recent studies on the elastic behaviour of single long DNA strands in buffer solutions have revealed how to make a fluid in which oscillatory viscoelastic convection might be observed. Recently, this notion was confirmed by Kolodner [21], who found oscillatory convection in DNA suspensions in annular geometry. Theoretically, these studies reignite interest in heat convection in viscoelastic fluids.
Sushila et. al. [25] studied a hybrid analytical algorithm for the thin film flow problem that arises in non-Newtonian fluid. They looked at the thin film flow of a third-grade fluid down an inclined plane in their paper. For the local fractional transport equation that occurs in fractal porous media, in [14], a an effective computational technique is presented. Mehta et. al. [22] investigated heat generation/absorption and the effect of joule heating on radiating MHD mixed convection stagnation point flow along vertical stretched sheet embedded in a permeable medium. The use of an unique fractional derivative in the analysis of heat and mass transfer for the slipping flow of viscous fluid with SWCNT's subject to Newtonian heating is explored by [17]. Whereas heat and mass transfer fractional second grade fluid with slippage and ramped wall temperature using Caputo-Fabrizio fractional derivative approach is investigated by [24].
Due to a variety of real-world situations where the Fourier law of heat flux is insufficient, the dynamics of Maxwell-Cattaneo (or non-fourier) fluids have drawn interest. In his investigation of the theory of gases, Maxwell argued that the relationship between heat flow and temperature gradient not only contain a finite relaxation time but also not be instantaneous. In the case of solid, Cattaneo [3] established a comparable relation, which Oldroyd [11] developed further. Later additions were important, such as those by Fox [20] and Carrassi, Morro[18]. The classical Fourier law of heat conduction expresses the heat flux within a medium is proportional to the local temperature gradient in the system. i.e.

$$V_T = -K\nabla T \tag{1}$$

In which V_T is heat flux, T is temperature and K the thermal conductivity. A well consequence of this law is that the heat purturbation propagate with a infinite velocity. To eliminate this unphysical feature, Maxwell-Cattaneo law is

one of the various modifications fourier law and takes the form:

$$\tau_T \frac{DV_T}{Dt} = -V_T - K\nabla T \tag{2}$$

Where the relaxation time is τ_T and the thermal conductivity is K. The derivative $\frac{D}{Dt}$ here represents the time derivative following the motion so that:

$$\frac{DV_T}{Dt} = \left(\frac{\partial}{\partial t} + V.\nabla\right) V_T \tag{3}$$

Where t is time and V is velocity. When a finite speed heatwave [6],[1],[2] is solved by the inclusion of finite relaxation periods, the parabolic heat equation of Fourier fluids, in which heat diffuses at infinite speed, is transformed into a hyperbolic heat equation. The significance of the thermal relaxation term is typically expressed by the dimensionless Maxwell-Cattaneo coefficient C_T, which is the ratio of the thermal relaxation time to twice the thermal diffusion time.

$$C_T = \frac{\tau_T K}{2\rho C_P d^2} = \frac{\tau_T \kappa}{2d^2} = \frac{\left(\frac{\tau_T}{2}\right)}{\tau_\kappa} \tag{4}$$

where thermal diffusion time is $\tau_\kappa (= \frac{d^2}{\kappa})$, density is ρ, specific heat at constant pressure is C_P, length is d and thermal diffusivity is κ. Thus the classical Fourier law has $C_T = 0$.

Numerous physical scenarios have been investigated when it comes to the Maxwell-Cattaneo heat transport effect, including nano-fluid and nano-material [7], biological tissue [26] and stellar interiors [16] in the context of DDC. Many factors, including the coefficient definition, affect the Maxwell-Cattaneo effect's potential importance. Eltayeb [9] discussed convection instabilities of Maxwell-Cattaneo fluids. In his study, he used three distinct forms of the time derivative of the heat flux to explore the linear and weakly nonlinear stabilities of a horizontal layer of fluid obeying the Maxwell-Cattaneo relationship of heat flux and temperature. While Eltayeb, Hughes, and Proctor [10] have examined the convection instability of a Maxwell-Cattaneo fluid in the presence of a vertical magnetic field and have discussed about the instability of a Benard layer under a vertical uniform magnetic field. The DDC of Maxwell-Cattaneo fluid has been studied by Hughes, Proctor and Eltayeb [8]. The consequences of include the Maxwell-Cattaneo (M-C) effects on the commencement of DDC, in which two factors alter the density of a fluid but diffuse at separate rates, were investigated in that study. For both temperature and salinity they considered Maxwell-Cattaneo effect. The modified salinity evolution equation is expressed as:

$$\tau_{\mathscr{C}} \frac{DV_{\mathscr{C}}}{Dt} = -V_{\mathscr{C}} - \kappa_{\mathscr{C}} \nabla \mathscr{C} \tag{5}$$

by analogy with temperature equation when M-C effect is included. where $\mathscr{C}$

is salt concentration, κ is salinity diffusivity, $\tau_{\mathscr{C}}$ the relaxation time for salinity and $V_{\mathscr{C}}$ is salt flux. Most of the above discussed work is related with the Newtonian fluid.
The onset of DDC in viscoelastic fluid (non-Newtonian fluid)layer is investigated by Malashetty and Swamy [19]. They analysed the stability of a binary viscoelastic fluid layer using linear and weakly nonlinear methods in that study. In view of importance viscoelastic fluid as discussed above, in this paper we carry out a linear stability analysis for a Maxwell-Cattaneo DDC in a viscoelastic fluid layer. Here, we focus on the scenario in which the M-C coefficients are extremely small, driven by geophysical and astrophysical concerns. Therefore, even when $C_T, C_S << 1$, new mechanisms for oscillatory instability might develop, given that the initial gradients of temperature and salinity are relatively significant. This is because the modified equations now describe singular perturbations in the time domain.
The work is presented in the following way. The physical problem is discussed in sect. 2 with a brief mathematical formulation. In sect. 3, the linear stability analysis in oscillatory convection for two cases i.e ($C_T = 0$ and $C_S = 0$) for the free-free boundaries is covered. The results and discussion are included in sect. 4, where we described results shown with the help of graph drawn for different parameters by fixing the values of all other parameters and discussed whether these parameters stabilise or destabilise the system. Last but not least, sect. 5 brings to a close a few key aspects of the analysis.

2 Mathematical model

2.1 The physical domain

We consider DDC in a horizontal layer of an incompressible binary viscoelastic Maxwell-Cattaneo fluid confined between two parallel horizontal planes at $z = 0$ and $z = \mathrm{d}$, a distance d apart with the vertically downward gravity g acting on it. Origin is set in the lower boundary of a Cartesian frame of reference, horizontal component x and vertical component z increases upwards. The surfaces are stretched indefinitely in both x and y directions while maintaining a consistent temperature gradient ΔT across the porous layer. To account for the impact of density fluctuations, we presum that the Oberbeck-Boussinesq approximation is used.

2.2 Governing equations

The momentum equation is modelled using the viscoelastic fluid of the Oldroyd type. The basic governing equations are

$$\left(1+\lambda_1\frac{\partial}{\partial t}\right)\left[\rho_0\left(\frac{\partial V}{\partial t}+V.\nabla V\right)+\nabla p-\rho g\right]=\mu\left(1+\lambda_2\frac{\partial}{\partial t}\right)\nabla^2 V \quad (6)$$

$$\left(\frac{\partial T}{\partial t} + (V.\nabla)T\right) = -\nabla.V_T \tag{7}$$

$$\tau_T\left(\frac{\partial U_T}{\partial t} + \nabla.(VU_T)\right) = -U_T - K\nabla^2 T \tag{8}$$

$$\left(\frac{\partial \mathscr{C}}{\partial t} + (V.\nabla)\mathscr{C}\right) = -\nabla.V_{\mathscr{C}} \tag{9}$$

$$\tau_{\mathscr{C}}\left(\frac{\partial U_{\mathscr{C}}}{\partial t} + \nabla.(VU_{\mathscr{C}})\right) = -U_{\mathscr{C}} - K_{\mathscr{C}}\nabla^2\mathscr{C} \tag{10}$$

$$\nabla.V = 0 \tag{11}$$

where $U_T = \nabla.V_T$, $U_{\mathscr{C}} = \nabla.V_{\mathscr{C}}$, $V = (u, v, w)$ is velocity, μ is viscosity, λ_1 is relaxation parameter, λ_2 is retardation parameter, ρ is density, K is thermal conductivity, $K_{\mathscr{C}}$ is salt conductivity, V_T is heat flux and $V_{\mathscr{C}}$ is salt flux. The formula for the relationship between reference density, temperature, and salinity is:-

$$\rho = \rho_0\left[1 - \beta_T(T - T_0) + \beta_{\mathscr{C}}(\mathscr{C} - \mathscr{C}_0)\right] \tag{12}$$

Temperature and salinity's appropriate boundary conditions are:-

$$T = T_0 + \Delta T \text{ at } z = 0 \text{ and } T = T_0 \text{ at } z = d \tag{13}$$

$$\mathscr{C} = \mathscr{C}_0 + \Delta\mathscr{C} \text{ at } z = 0 \text{ and } \mathscr{C} = \mathscr{C}_0 \text{ at } z = d \tag{14}$$

2.3 Initial state

It is considered that the fluid is in a quiescent initial state, which is represented by

$$V_b = (0,0,0), P = P_b(z), T = T_b(z), \mathscr{C} = \mathscr{C}_b(z), \rho = \rho_b(z), \quad V_{T_b} = (0,0,V_T(z)), V_{\mathscr{C}_b} = (0,0,V_{\mathscr{C}}(z)) \tag{15}$$

Using (2.3) in Eqs. (6) − (12) yield

$$\frac{dp_b}{dz} = -\rho_b g, \frac{d^2T_b}{dz^2} = 0, \frac{d^2\mathscr{C}_b}{dz^2} = 0 \tag{16}$$

The initial state solution for temperature and salinity fields are given by:-

$$T_b(z) = T_l - \Delta T\frac{z}{d}, \mathscr{C}_b(z) = \mathscr{C}_l - \Delta\mathscr{C}\frac{z}{d} \tag{17}$$

2.4 Perturbed state

On the initial state, we superimpose a disturbance of the type:-

$$\begin{aligned} V = V_b(z) + V'(x, y.z, t), T = T_b(z) + T'(x, y, z.t), \mathscr{C} = \mathscr{C}_b(z) + \mathscr{C}'(x, y, z, t), \\ P = P_b(z) + P'(x, y, z, t), \rho = \rho_b(z) + \rho'(x, y, z, t), V_T = V_{T_b} + V'_T(x, y, z, t), \\ V_{\mathscr{C}} = V_{\mathscr{C}_b} + V'_{\mathscr{C}}(x, y, z, t) \end{aligned} \tag{18}$$

where perturbations are indicated by primes. Introducing (18) in Eqs. (6) – (11), and using basic state from Eq. (16), The resulting equations are then non-dimensionalized using the following transformations

$$(x, y, z) = d(x^*, y^*, z^*), t = \frac{d^2}{\kappa_{Tz}} t^*, \lambda_1 = \frac{\kappa_{Tz}}{d^2}\lambda_1 *, (V') = \frac{\kappa_{Tz}}{d}(V^*), P' = \frac{\mu \kappa_{Tz}}{K_z} P^*,$$

$$\lambda_2 = \frac{\kappa_{Tz}}{d^2}\lambda_2 *, V_T = \Delta T \frac{K}{d} V_T^*, V_{\mathscr{C}} = \Delta T \frac{\kappa}{d} V_{\mathscr{C}}^*, T' = (\Delta T) T^*, \mathscr{C}' = (\Delta \mathscr{C}) \mathscr{C}^* \tag{19}$$

After eliminating the asterisks for simplicity, we arrived at the non-dimensional, linear governing equations, which are

$$\left(1 + \lambda_1 \frac{\partial}{\partial t}\right)\left[\frac{1}{Pr}\frac{\partial}{\partial t}\nabla^2 V - Ra_T \nabla_1^2 T + Ra_S \nabla_1^2 \mathscr{C}\right] - \left(1 + \lambda_2 \frac{\partial}{\partial t}\right)\nabla^4 V = 0 \tag{20}$$

$$\frac{\partial T}{\partial t} = w - U_T \tag{21}$$

$$2C_T \frac{\partial U_T}{\partial t} = -U_T - \nabla^2 T \tag{22}$$

$$\frac{\partial \mathscr{C}}{\partial t} = w - U_{\mathscr{C}} \tag{23}$$

$$2C_S \frac{\partial U_{\mathscr{C}}}{\partial t} = -U_{\mathscr{C}} - \tau \nabla^2 \mathscr{C} \tag{24}$$

where the Prandtl number Pr, thermal Rayleigh number Ra_T, solutal Rayleigh number Ra_S, Diffusivity ratio τ, Maxwell-Cattaneo coefficient for temperature C_T and Maxwell-Cattaneo coefficient for salinity $C_{\mathscr{C}}$ are defined as: $Pr = \frac{\nu}{\kappa_{T_Z}}$, $Ra_T = \frac{\beta_T g \Delta T d K_Z \nu}{\kappa_{T_Z}}$, $Ra_S = \frac{\beta_S g \Delta \mathscr{C} d K_Z \nu}{\kappa_{T_Z}}$, $\tau = \frac{\kappa_{\mathscr{C}}}{\kappa}$, $C_T = \frac{\tau_T \kappa}{2d^2}$, $C_S = \frac{\tau_{\mathscr{C}} \kappa_{\mathscr{C}}}{2d^2}$, and u, v and w are x, y and z component of velocity respectively.
The boundaries are assumed to be impermeable, isothermal and stress free, therefore we have the following conditions

$$w = \frac{\partial^2 w}{\partial z^2} = T = \mathscr{C} = 0 \text{ at } z = 0, 1. \tag{25}$$

3 Linear Stability Analysis

In this part, we employ linear theory to forecast the thresholds of both marginal and oscillatory convections. Assuming that the amplitudes are small enough, the time-dependent periodic disturbances in a horizontal plane are used to solve the eigenvalue problem specified by Eqs. (20)–(24) subject to the boundary conditions (20) is solved as follows:

$$\begin{pmatrix} w \\ T \\ \mathscr{C} \\ U_T \\ U_{\mathscr{C}} \end{pmatrix} = \begin{pmatrix} W(z) \\ \Theta(z) \\ \Phi(z) \\ \zeta(Z) \\ \gamma(Z) \end{pmatrix} e^{i(lx+my)+\sigma t} \tag{26}$$

where the growth rate is represented by the complex quantity σ and the horizontal wave numbers l and m. W, Θ, Φ, ζ and γ are the amplitudes of stream function, temperature field, solute field, heat flux and solute flux respectively.

$$\left[(1+\lambda_1\sigma)\left(\frac{\sigma}{Pr}(D^2-a^2)\right)+(1+\lambda_2\sigma)(D^2-a^2)^2\right]W+(1+\lambda_1\sigma)Ra_Ta^2\Theta \\ -(1+\lambda_1\sigma)Ra_Sa^2\Phi=0 \tag{27}$$

$$-W+\sigma\Theta+\zeta=0 \tag{28}$$

$$(D^2-a^2)\Theta+(2C_T\sigma+1)\zeta=0 \tag{29}$$

$$-W+\sigma\Phi+\gamma=0 \tag{30}$$

$$\tau(D^2-a^2)\Phi+(2C_S\sigma+1)\gamma=0 \tag{31}$$

where $D=\frac{d}{dz}$ and $a^2=l^2+m^2$. on the free boundary. we take the solution of Eqn. (27)-(31) satisfying the boundary condition for free-free case:

$$[W(z),\Theta(z),\Phi(z),\zeta(z),\gamma(z)]=[W_0,\Theta_0,\Phi_0,\zeta_0,\gamma_0]\sin(n\pi z),(n=1,2,3,...) \tag{32}$$

Substituting Eq. (32) into (27)-(31), and considering $n=1$, we get a matrix equation

$$\begin{bmatrix} M_1 & -a^2Ra_T & a^2Ra_S & 0 & 0 \\ -1 & \sigma & 0 & 1 & 0 \\ 0 & -\alpha & 0 & 2C_T\sigma+1 & 0 \\ -1 & 0 & \sigma & 0 & 1 \\ 0 & 0 & -\tau\alpha & 0 & 2C_S\sigma+1 \end{bmatrix} \begin{bmatrix} W_0 \\ \Theta_0 \\ \Phi_0 \\ \zeta_0 \\ \gamma_0 \end{bmatrix} = \begin{bmatrix} 0 \\ 0 \\ 0 \\ 0 \\ 0 \end{bmatrix} \tag{33}$$

where $\alpha=a^2+\pi^2$, $M_1=\left[\frac{-\sigma}{Pr}+\frac{(1+\lambda_2\sigma)\alpha}{(1+\lambda_1\sigma)}\right]\alpha$.

For non-trivial solution of W, Θ, Φ, ζ and γ, we need to make the determinant of the above matrix as zero, we get

$$Ra_T=\left(\sigma+\frac{\alpha}{(2C_T\sigma+1)}\right)\left[\frac{M_1}{a^2}-\frac{Ra_S(2C_S\sigma+1)}{\sigma(2C_S\sigma+1)+\tau\alpha}\right] \tag{34}$$

3.1 Stationary state

We have $\sigma = 0$ at the stability margin for the direct bifurcation, or stable onset. The Rayleigh number at which a marginally stable steady mode occurs therefore becomes

$$Ra_T^{st} = \frac{\alpha^3}{a^2} - \frac{Ra_S}{\tau} \tag{35}$$

We obtained the result which is comparable to that of Turner [13]. This result also indicate that stationary Rayleigh number is independent of the viscoelastic parameters and Maxwell-Cattaneo coefficients. The stationary Rayleigh number Ra_T^{st} given by Eq. (35) attains the critical value

$$Ra_{T,C}^{st} = \frac{27}{4}\pi^4 - \frac{Ra_S}{\tau} \tag{36}$$

for the wave number $a_c = \frac{\pi}{\sqrt{2}}$.
When $Ra_S = 0$, Eq. (36) gives

$$Ra_{T,C}^{st} = \frac{27}{4}\pi^4 \tag{37}$$

which is classical outcome of Newtonian fluid layer mentioned in the book of Chandrashekhar [23].

3.2 Oscillatory motion

In general, σ, the growth rate, is a complex quantity with the formula $\sigma = \sigma_r + i\omega$. While the system will become unstable for $\sigma_r > 0$, it is always stable for $\sigma_r < 0$. $\sigma_r = 0$ for the neutral stability state.

1. The case of C_S=0

we put C_S=0 in Eq. (34), and get

$$Ra_T = \left(\sigma + \frac{\alpha}{2C_T\sigma + 1}\right)\left[\left(\frac{-\sigma\alpha}{Pra^2} + \frac{(1+\lambda_2\sigma)\alpha^2}{(1+\lambda_1\sigma)a^2}\right) - \frac{Ra_S}{\sigma + \tau\alpha}\right] \tag{38}$$

then put $\sigma = i\omega$(ω is real) in Eq. (38) and get

$$Ra_T = \Pi_1 + (i\omega)\,\Pi_2 \tag{39}$$

The expression for Π_1 is given by

$$\Pi_1 = D_1 - D_2 - D_3 + D_4 - D_5$$

The fact that Ra_T is a physical quantity proves that it is real. Hence, from Eq. (39) it follows that either $\omega = 0$ (steady onset) or $\Pi_2 = 0$ ($\omega \neq 0$, oscillatory onset). For oscillatory onset $\Pi_2 = 0(\omega \neq 0)$ and this provides a dispersion relation of the form

$$B_1\left(\omega^2\right)^3 + B_2\left(\omega^2\right)^2 + B_3\left(\omega^2\right) + B_4 = 0 \tag{40}$$

where the constants $B_1 = Q_1, B_2 = Q_1Q_7 + Q_2 - Q_3Q_5 - Q_3Q_8, B_3 = Q_2Q_7 - Q_4Q_5 - Q_3Q_6 - Q_3Q_7Q_8 - Q_4Q_8 + Q_9 + Q_3Q_{10}, B_4 = -Q_4Q_6 - Q_4Q_7Q_8 + Q_7Q_9 + Q_4Q_{10}$

Now Eq. (39) with $\Pi_2 = 0$, gives oscillatory Rayleigh number Ra_T^{osc} at the margin of stability as

$$Ra_T^{osc} = \Pi_1. \tag{41}$$

Also, to cause the oscillatory convection, ω^2 must be positive. The symbols $D_1, D_2, D_3, D_4, D_5, Q_1, Q_2, Q_3, Q_4, Q_5, Q_6, Q_7, Q_8, Q_9, Q_{10}, Q_{11}, Q_{12}, Q_{13}, Q_{14}$, Q_{15}, Q_{16} and Π_2 are defined in Appendix-I

2. The case of C_T=0

we put C_T=0 in Eq. (34), and get

$$Ra_T = (\sigma + \alpha)\left[\left(\frac{-\sigma\alpha}{Pra^2} + \frac{(1+\lambda_2\sigma)\alpha^2}{1+\lambda_1\sigma)a^2}\right) - \frac{Ra_S(2C_S\sigma+1)}{(\sigma(2C_S\sigma+1)+\tau\alpha)}\right] \tag{42}$$

then put $\sigma = i\omega(\omega$ is real) in Eq. (42) and get

$$Ra_T = \Pi_1' + (i\omega)\,\Pi_2' \tag{43}$$

The expression for Π_1' is given by

$$\Pi_1' = F_1 - F_2 + F_3 + F_4 - F_5$$

For oscillatory onset $\Pi_2' = 0$ ($\omega \neq 0$) and this provides a dispersion relation of the form

$$C_1\left(\omega^2\right)^3 + C_2\left(\omega^2\right)^2 + C_3\left(\omega^2\right) + C_4 = 0 \tag{44}$$

where the constants $C_1 = P_1P_6^2 - P_2P_6^2P_7$, $C_2 = P_1 + 2P_2P_5P_6P_7 - P_2P_7 - P_3P_6^2P_7 + P_6^2P_8 + P_2P_6P_9$, $C_3 = P_1P_5^5 - 2P_1P_5P_6 - P_2P_4 - P_2P_5^2P_7 + 2P_3P_5P_6P_7 - P_3P_7 - 2P_5P_6P_8 + P_8 - P_2P_5P_9 + P_3P_6P_9 + P_2P_9$, $C_4 = -P_3P_4 - P_3P_5^2P_7 + P_5^2P_8 - P_3P_5P_9 + P_3P_9$

Now Eq. (43) with $\Pi_2' = 0$, gives oscillatory Rayleigh number Ra_T^{osc} at the margin of stability as

$$Ra_T^{osc} = \Pi_1'. \tag{45}$$

Also, to cause the oscillatory convection, ω^2 must be positive. The symbols $F_1, F_2, F_3, F_4, F_5, P_1, P_2, P_3, P_4, P_5, P_6, P_7, P_8, P_9, P_{10}, P_{11}, P_{12}, P_{13}, P_{14}$ and Π_2' are defined in Appendix-I

4 Result and discussion

In this paper, Linear stability has been investigated in the presence of Maxwell-Cattaneo DDC for viscoelastic fluid. The onset of instability is examined for various controlling parameters such as Prandtl number (Pr), diffusivity ratio (τ),

relaxation parameter(λ_1), retardation parameter (λ_2), solutal Rayleigh number (Ra_S), Maxwell-Cattaneo coefficient for temperature (C_T) and Maxwell-Cattaneo coefficient for salinity (C_S). In most physical contexts, the Maxwell-Cattaneo effect is so negligible that we have concentrated on the case where C is smaller than 1, where C is used in the discussion to signify either C_T or C_S. Because C is so small, the Maxwell-Cattaneo effect only manifests itself for concomitantly strong heat and salinity gradients.

In the (a, Ra_T) plane, Fig. 1(a)-(f) illustrate the neutral curves of oscillatory convection for C_S, λ_1, λ_2, τ, Pr and Ra_S when $C_T = 0$ while Fig 1(a')-(f') illustrate the neutral curves when $C_S = 0$ for C_T, λ_1, λ_2, τ, Pr and Ra_S. Fig. 1(a) illustrates how C_S affects the system's stability whereas the impact of C_T is depicted in Fig. 1(a'). With a rise in C_S, the minimum Rayleigh number increases, but with a rise in C_T, the minimum Rayleigh number decreases. So, clearly it is shown that C_S has stabilizing while C_T has destabilizing effect on the stability of the system.

Fig. 1(b) and Fig. 1(b') show the influence of relaxation parameter λ_1 on the stability of the system for $C_T = 0$ and $C_S = 0$ respectively. We can see that raising λ_1 causes the lowest value of the Rayleigh number, Ra_T, is decreases, indicating that λ_1 has a destabilising influence on the Maxwell-Cattaneo DDC in viscoelastic fluid for both situations, where ($C_T = 0$ and $C_S = 0$). Also, it is shown graphically that for different values of λ_1 the case $C_S = 0$ is more stable as compare to $C_T = 0$. Fig. 1(c) and Fig. 1(c') demonstrate that when the value of λ_2 grows, the lowest Rayleigh number similarly rises, stabilising the system. For different values of λ_2, $C_S = 0$ case is more stable. Viscoelastic parameter behaviour is clear and consistent with what [12] said.

The influence of diffusion ratio τ on the system's stability is depicted in Fig 1(d) for $C_T = 0$ and in Fig 1(d') for $C_S = 0$. It is shown the minimum of critical Rayleigh number rises with rise in the value of (τ). It occurs because $\tau = \frac{\kappa_{\mathscr{C}}}{\kappa}$ has an inverse relationship to thermal diffusivity κ. Therefore, when the diffusivity ratio τ increases, the value of thermal diffusivity falls, implying an increase in the Rayleigh number. Also, for different values of τ, $C_S = 0$ is more stable.

Fig 1(e) and Fig 1 (e') show graphs for various values of Prandtl number Pr when $C_T = 0$ and $C_S = 0$ respectively. For the case $C_T = 0$, the system becomes stabilised as a result of the minimum of Ra_T value increasing together with the value of Prandtl number Pr. The fact that Pr is inversely proportional to thermal diffusivity explains it. It has been demonstrated that as the value of Pr increases, the minimum Rayleigh number drops and the system becomes unstable as a result for $C_S = 0$.

The graphs for various Ra_S values on the (a, Ra_T) plane for $C_T = 0$ and $C_S = 0$ are shown in Fig 1(f) and Fig 1(f') respectively. So, for $C_T = 0$, as Ra_S values rise, the minimum of Rayleigh number rises as well, which causes the system to stabilise. It has been seen that the system becomes unstable when the value of Ra_S rises because the minimum Rayleigh number decreases for $C_S = 0$.

5 Conclusion

We have attempted to understand the onset of Maxwell-Cattaneo DDC in a binary viscoelastic fluid layer. With the use of the normal mode technique, linear stability analysis for stationary and oscillatory convection is carried out in this study. Because the Maxwell-Cattaneo coefficients have no effect on stationary states, we have generated graphs for oscillatory convection rather than stationary convection.
The conclusions are as follows.

1. The onset of oscillatory convection is found to be delayed by C_S, λ_2, τ, Pr, and Ra_S, whereas the onset of oscillatory convection is found to be advanced by increasing the value of λ_1, which decreases the value of Rayleigh number corresponding to oscillaory convection in the case of $C_T = 0$.

2. λ_2, τ are found to delay the onset of oscillatory convection whereas on increasing the value of C_T, λ_1, Pr and Ra_S the value of Rayleigh number corresponding to oscillaory convection decreases, thus it advances the onset of convection for the case $C_S = 0$.

According to Maxwell-Cattaneo law, there is currently relatively limited study being done on thermal instability. The Maxwell-Cattaneo law for heat flux and temperature relation with various external effects, such as Electrohydrodynamics, radiation, rotation, etc., can therefore be applied to diverse types of fluids in the future.

Appendix-I

$D_1 = \omega^2 Q_8 \left(1 - \frac{Q_{11}}{Q_{16}\omega^2+1}\right)$, $D_2 = \frac{\omega^2 Q_{12}}{Q_3\omega^2+Q_4}\left(1 - \frac{Q_{11}}{Q_{16}\omega^2+1}\right)$, $D_3 = \frac{\omega^2 Q_{13}}{Q_7+\omega^2}\left(1 - \frac{Q_{11}}{Q_{16}\omega^2+1}\right)$, $D_4 = \frac{\omega^2 Q_{14}}{(Q_3\omega^2+Q_4)(Q_{16}\omega^2+1)}$, $D_5 = \frac{Q_5}{(Q_7+\omega^2)(Q_{16}\omega^2+1)}$, $Q_1 = 4C_T^2\alpha^2\lambda_1\lambda_2$, $Q_2 = \lambda_1\lambda_2\alpha^2 - 2C_T\lambda_1\lambda_2\alpha^2$, $Q_3 = \lambda_1^2 a^2$, $Q_4 = a^2$, $Q_5 = 4Ra_S C_T^2\tau\alpha$, $Q_6 = Ra_S\tau\alpha - 2C_T Ra_S\tau\alpha$, $Q_7 = \tau^2\alpha^2$, $Q_8 = \frac{\alpha}{Pra^2}$, $Q_9 = \alpha^3(\lambda_2-\lambda_1)$ $Q_{10} = \alpha Ra_S$, $Q_{11} = 2C_T$, $Q_{12} = (\lambda_2 - \lambda_1)\alpha^2$, $Q_{13} = Ra_S$, $Q_{14} = \alpha^3\lambda_1\lambda_2$, $Q_{15} = Ra_S\tau\alpha^2$, $Q_{16} = 4C_T^2$, $\Pi_2 = \frac{(Q_1\omega^4+Q_2\omega^2)}{(Q_3\omega^2+Q_4)} - \frac{(Q_5\omega^2+Q_6)}{Q_7+\omega^2} - Q_8 + \frac{Q_9}{(Q_3\omega^2+Q_4)} + \frac{Q_{10}}{(Q_7+\Omega^2)}$, $F_1 = \omega^2 P_{10}$, $F_2 = \frac{P_{11}\omega^2}{P_2\omega^2+P_3}$, $F_3 = \frac{\omega^2 Q_{13}((Q_5-Q_6\omega^2)-1)}{(Q_5-Q_6\omega^2)^2+\omega^2}$, $F_4 = \frac{\omega^2 Q_{12}}{Q_2\omega^2+Q_3}$, $F_5 = \frac{Q_9+Q_4(Q_5-Q_6\omega^2)}{(Q_5-Q_6\omega^2)^2+\omega^2}$, $P_1 = \alpha^2\lambda_1\lambda_2$, $P_2 = a^2\lambda_1^2$, $P_3 = a^2$, $P_4 = Ra_S\tau\alpha$, $P_5 = \tau\alpha$, $P_6 = 2C_S$, $P_7 = \frac{\alpha^2}{Pra^2}$, $P_8 = (\lambda_2 - \lambda_1)\alpha^3$, $P_9 = 2Ra_S\alpha C_S$, $P_{10} = \frac{\alpha}{a^2 Pr}$, $P_{11} = (\lambda_2 - \lambda_1)\alpha^2$, $P_{12} = \alpha^3\lambda_1\lambda_2$, $P_{13} = 2C_S Ra_S$, $P_{14} = Ra_S\alpha$, $\Pi_2' = \frac{P_1\omega^2}{P_2\omega^2+P_3} - \frac{P_4}{(P_5-P_6\omega^2)^2+\omega^2} - P_7 + \frac{P_8}{P_2\omega^2+P_3} - \frac{P_9((P_5-P_6\omega^2)-1)}{(P_5-P_6\omega^2)^2+\omega^2}$

Acknowledgment

Author, Monal Bharty, sincerely thanks Central University of Jharkhand for providing financial support in the form of a research fellowship. This work is only presented in the 5th International Conference on Mathematical Modelling,

Applied Analysis and Computation-2022 (ICMMAAC-22) held in JECRC University, Jaipur (India).

References

[1] B. Straughan, *Heat waves*, New York, NY: Springer, 2011.

[2] B. Straughan, Tipping points in Cattaneo-Christov thermohaline convection, *Proc. R. Soc. A*, 467, 7–18 (2011).

[3] C. Cattaneo, Sulla conduzione del calore, *Atti Mat. Fis. Univ. Modena*, 3, 83–101 (1948).

[4] C.W. Horton, F.T. Rogers, Convection currents in a porous medium. *J. Appl. Phys.*, 16, 367-370 (1945).

[5] C.M. Vest, V.S. Arpaci, Overstability of a viscoelastic fluid layer heated from below, *J.Fluid Mech*, 36, 613-623 (1969).

[6] D.D. Joseph, L.Preziosi, Heat waves, *Rev.Mod. Phys.*, 61, 41–73 (1989).

[7] D. Jou, A. Sellitto, FX. Alvarez, Heat waves and phonon-wall collisions, *nanowires. Proc. R. Soc. A*, 467, 2520–2533 (2011).

[8] D.W. Hughes, M.R.E. Proctor, I.A. Eltayeb, Maxwell–Cattaneo double-diffusive convection:limiting cases, *J. Fluid Mech.*, vol. 927 (2021).

[9] I. A. Eltayeb, Convective instabilities of Maxwell–Cattaneo fluids, *Proc. R. Soc. A*, 473 (2017) https://doi.org/10.1098/rspa.2016.0712

[10] I. A. Eltayeb, D. W. Hughes, M. R. E. Proctor, The convective instability of a Maxwell–Cattaneo fluid in the presence of a vertical magnetic field, *Proc. R. Soc. A*, 476 (2020) https://doi.org/10.1098/rspa.2020.0494

[11] J.G. Oldroyd, On the formulation of rheological equations of state, *Proc. R. Soc. Lond. A*, 200, 523–541 (1950).

[12] J. Kang, Fu, Ceji. Fu, W. Tan, Thermal convective instability of viscoelastic fluids in a rotating porous layer heated from below, *J. Non-Newtonian Fluid Mechanics*, 166, 93-101 (2011).

[13] J.S. Turner, *Buoyancy Effects in Fluids*, Cambridge University Press, London, 1973.

[14] J. Singh, An efficient computational method for local fractional transport equation occurring in fractal porous media, *Comput. Appl. Math*, 39, 137(2020).

[15] J.Zhou, I. Papautsky, Viscoelastic microfluidics: progress and challenges, *Microsyst and Nanoeng*, 6, 1-24 (2020).

[16] L. Herrera, N. Falcón, Heat waves and thermohaline instability in a fluid, *Phys. Lett. A*, 201, 33–37 (1995).

[17] M. Ahmad, M. I. Asjad, J. Singh, Application of novel fractional derivative to heat and mass transfer analysis for the slippage flow of viscous fluid with SWCNT's subject to Newtonian heating, *Math. Methods Appl. Sci*, (2021) https://doi.org/10.1002/mma.7332

[18] M. Carrassi, A. Morro, A modified Navier-Stokes equation, and its consequences on sound dispersion, *Nuovo Cimento B*, 9, 321–343 (1972).

[19] M.S. Malashetty, M. Swamy, The onset of double diffusive convection in a viscoelastic fluid layer, *Int. J. Non Newtonian Fluid Mech.*, vol. 165, 1129-1138 (2010).

[20] N. Fox, Low temperature effects and generalized thermoelasticity, *IMA J. Appl. Maths*, 5, 373–386 (1969).

[21] P. Kolodner, Oscillatory convection in viscoelastic DNA suspensions, *J.Non- Newtonian Fluid Mech*, 75, 167–192 (1998).

[22] R. Mehta, R. Kumar, H. Rathore, J. Singh, Joule heating effect on radiating MHD mixed convection stagnation point flow along vertical stretching sheet embedded in a permeable medium and heat generation/absorption, *Heat Transfer (Wiley)*, 51(8), 7369-7386 (2022).

[23] S. Chandrasekhar, *Hydrodynamic and Hydromagnetic Stability*, Dover, New York, 1981.

[24] S. U. Haq, S. U. Jan, S. I. A. Shah, I. Khan, J. Singh, Heat and mass transfer of fractional second grade fluid with slippage and ramped wall temperature using Caputo-Fabrizio fractional derivative approach, *AIMS Mathematics*, 5(4), 3056-3088 (2020).

[25] Sushila, J. Singh, D. Kumar, D. Baleanu, A hybrid analytical algorithm for thin film flow problem occurring in non-Newtonian fluid mechanics, *Ain Shams Eng. J*, 12(2), 2297-2302 (2021).

[26] W. Dai, H. Wang, PM. Jordan, RE. Mickens, A. Bejan, A mathematical model for skin burn injury induced by radiation heating, *Int. J. Heat Mass Transfer*, 51, 5497–5510 (2008).

Figure 1: Oscillatory neutral stablity curves for different values of: 1(a) Maxwell-Cattaneo coefficient for solute C_S when $C_T = 0$; 1(a') Maxwell-Cattaneo coefficient for temperature C_T when $C_S = 0$.

Figure 2: Oscillatory neutral stability curves for different values of: 1(b) relaxation parameter λ_1 when $C_T = 0$; 1(b') relaxation parameter λ_1 when $C_S = 0$.

Figure 3: Oscillatory neutral stability curves for different values of: 1(c) retardation parameter λ_2 when $C_T = 0$; 1(c') retardation parameter λ_2 when $C_S = 0$.

Figure 4: Oscillatory neutral stability curves for different values of: 1(d) diffusivity ratio τ when $C_T = 0$; 1(d') diffusivity ratio τ when $C_S = 0$.

Figure 5: Oscillatory neutral stability curves for different values of: 1(e) Prandtl number Pr when $C_T = 0$; 1(e') Prandtl number Pr when $C_S = 0$.

Figure 6: Oscillatory neutral stability curves for different values of: 1(f) solutal Rayleigh number Ra_S when $C_T = 0$; 1(f') solutal Rayleigh number Ra_S when $C_S = 0$.

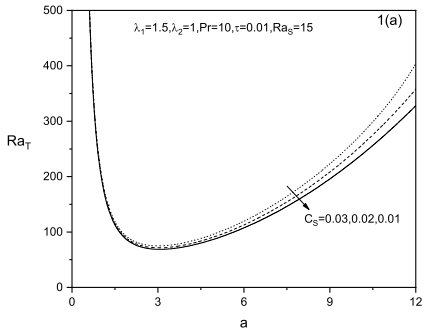

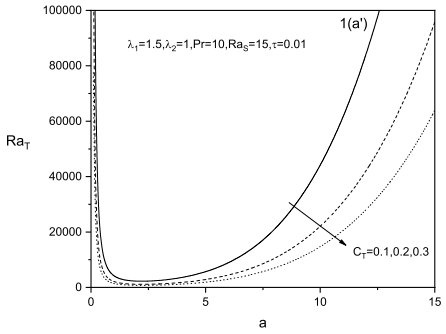

Figure 1

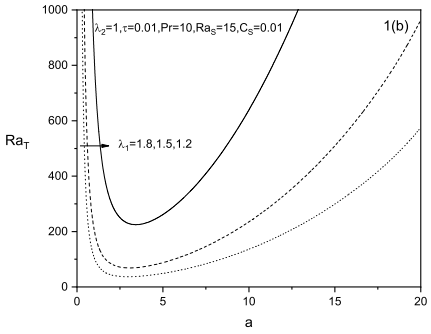

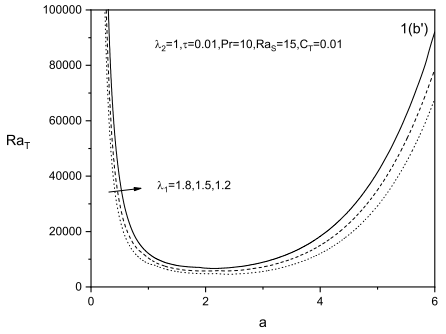

Figure 2

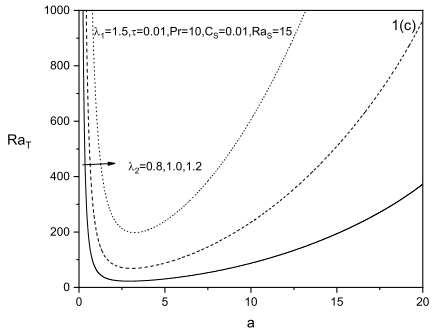

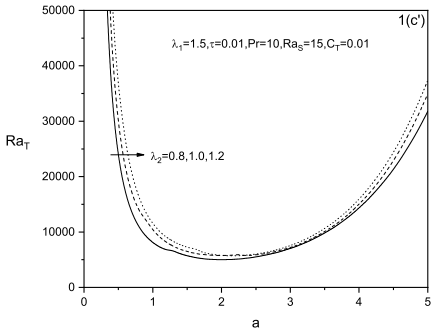

Figure 3

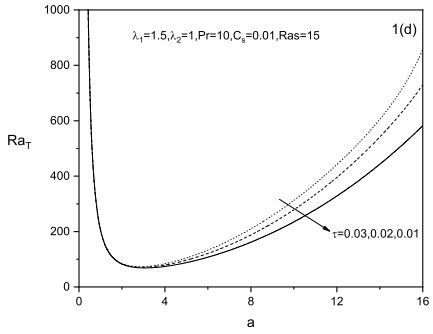

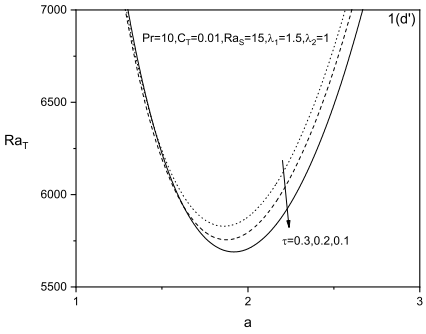

Figure 4

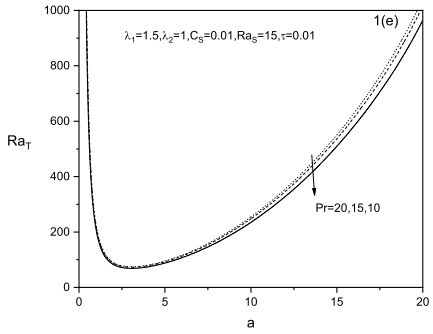

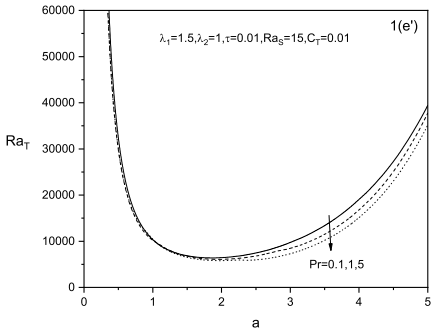

Figure 5

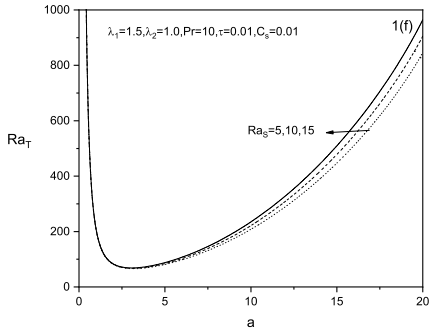

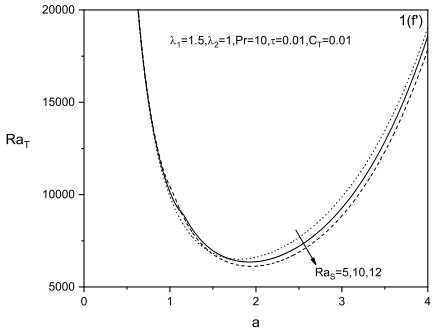

Figure 6